Proceedings of the ASME 2015 Dynamic Systems and Control Conference
DSCC2015
October 28-30, 2015, Columbus, Ohio, USA

DSCC2015-9979

PROPORTIONAL SEMG BASED ROBOTIC ASSISTANCE IN AN ISOLATED WRIST MOVEMENT

Edward J. Artz, Amy A. Blank, Marcia K. O'Malley
Mechatronics and Haptic Interfaces Lab
Department of Mechanical Engineering
Rice University
Houston, Texas, 77005
Email: eja2@rice.edu, amy.a.blank@rice.edu, omalleym@rice.edu

ABSTRACT

Numerous studies have demonstrated the efficacy of robots for motor therapy. Surface electromyography (sEMG) is appealing for user intent detection as the signal relates the individual's desired muscle contractile force. A drawback to sEMG interfaces is subject- and session-dependent calibration. We sought to investigate the effect of a simple sEMG assistive controller on user performance in the MAHI Exo-II, therapeutic exoskeleton. Agonist-antagonist muscles were related after normalization based on sub-maximal isometric contraction. Six subjects performed a target tracking task with four levels of assistance in wrist flexion-extension. Performance metrics were mean absolute position error and estimated muscular activity. In low levels of assistance, subject performance was not significantly affected, while increasing the assistance resulted in higher position errors. In characterizing the performance assistance trade-off, we better understand the capabilities of this simple controller. This investigation validates the feasibility of using a proportional control scheme for a therapeutic wrist exoskeleton system and motivates further testing with impaired subjects to optimize the system for use in a clinical setting.

INTRODUCTION

Spinal cord injury (SCI) is a common cause of disability in the United States with approximately 12,000 new instances of SCI each year. A large portion, 59.3%, of these individuals experience incomplete SCI [1]. In these individuals, there is a prospect for increasing motor function through intensive rehabilitation that promotes neuroplasticity, or the ability of the nervous system to reorganize in response to external stimuli [2].

Figure 1. THE MAHI EXO-II, AN UPPER-EXTREMITY THERAPEUTIC EXOSKELETON FOR REHABILITATION OF NEUROLOGICAL INJURY.

To improve motor therapy outcomes, numerous groups have proposed and employed robotic systems for rehabilitation as summarized in [3]. Robots, like the MAHI Exo-II (Figure 1), possess certain strengths making them well suited to a therapeutic role following neurological injury. They are capable of providing consistent, high intensity training, which improves therapeutic outcomes [4]. Clinicians, using the same sensors employed for robot control, can objectify subject performance using movement metrics that reflect scores in tradition clinical assessments [5]. Several studies have demonstrated an improvement in clinical measures of motor function following intervention with a robotic rehabilitation protocol in incomplete SCI subjects [6, 7].

Patient engagement is crucial during rehabilitation. When compared to protocols with actively engaged subjects, passive movements have lower therapeutic outcomes [8]. While some control schemes only require the patient to initiate movement, then complete the rest of the movement without user input, continuous control schemes offer benefits to rehabilitation in requiring user engagement. A primary challenge in employing robots for neurorehabilitation is discerning user intent. Different approaches have included impedance, electroencephalography, and surface electromyography (sEMG) based control schemes as summarized in [9].

Since the sEMG signal is related to muscle contractile forces, using sEMG in control of robotic systems provides insight into user intent. Further, sEMG interfaces offer benefits in accessing more impaired populations than impedance control schemes and preventing compensatory movements during therapy [10]. The relationship between sEMG and force is complex, however, as numerous factors influence the recorded sEMG signal. These factors include electrode placement, cross talk from nearby muscles, motor unit firing rate, number of motor units recruited, and stiffness of elastic biological elements such as tendons [11]. Many of these factors vary non-linearly with respect to movement velocity and joint position, among other variables, increasing the difficulty in modeling the force to sEMG relationship.

Different approaches have been taken to accurately model this relationship for continuous exoskeleton control, including artificial neural networks [12], neuro-fuzzy classifiers [13], and Hill model based approaches [14]. Many of these techniques are limited by intensive calibration procedures that are subject- and session-dependent and may require specialized EMG training [15]. The time dedicated to calibration may reduce time dedicated to active therapy in a clinical setting. A recent study in sEMG control investigated the trade-off between rudimentary sEMG control schemes with relaxed calibration procedures and subject performance [15]. They found that subjects possess the ability to adapt to an imprecise torque estimate, control the system effectively, and benefit from an assistive torque during elbow flexion-extension.

As a first step towards integration of sEMG for intent detection in robotic rehabilitation after incomplete SCI, we investigate a proportional control scheme for the MAHI Exo-II that would provide assistance in completing movements of the upper limb. Although proportional control has often been used in prosthetics (e.g., [16]), application to exoskeleton systems is complicated by the physical interaction between the user and the robot. Therefore, we sought to explore the effect of this control scheme on user performance with an exoskeleton. Specifically, we explored the effect of various levels of assistance from the developed controller on motion during a tracking task in wrist flexion-extension (FE) for healthy subjects when compared to back-driving the exoskeleton. It was postulated that subjects would be able to adapt quickly to the sEMG assistance, maintain performance, as measured by position error, and reduce observed muscular effort during the task as measured by the integral of EMG (iEMG), as previously observed for elbow flexion-extension [15]. This investigation validates the feasibility of the proposed control scheme in a wrist exoskeleton system and motivates further testing with impaired subjects to optimize the system for use in a clinical setting.

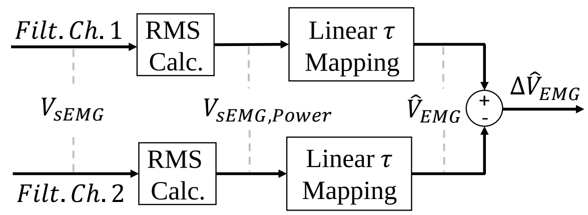

Figure 2. ACQUIRING THE SEMG CONTROL SIGNAL, WHERE V_{SEMG} ARE THE RECORDED AND FILTERED SEMG SIGNALS, $V_{SEMG,POWER}$ IS THE SIGNAL AFTER THE RUNNING RMS CALCULATION, $\hat{V}_{EMG}$ IS THE NORMALIZED SIGNAL, AND $\Delta\hat{V}_{EMG}$ IS THE DIFFERENCE IN AGONIST-ANTAGONIST NORMALIZED SIGNALS.

METHODS

The MAHI Exo-II Therapeutic Robotic Exoskeleton

The MAHI Exo-II, presented in [17], is a five DoF upper-extremity exoskeleton designed for rehabilitation following neurological injury. One DoF is passive allowing shoulder adduction-abduction for comfortable user fit. The four actuated DoF correspond to elbow flexion-extension, forearm pronation-supination, wrist FE, and wrist RU. Five DC motors (Maxon) coupled with capstan cable drive transmissions provide actuation. The cable drive system allows the user to back-drive the system without the backlash associated with gears and low inertia [18]. The wrist structure is a 3-RPS (revolute-prismatic-spherical) serial-in-parallel mechanism that allows rotation about the user's two wrist DoF for this experiment, flexion-extension and radial-ulnar deviation. For this experiment, all other DoF were held constant.

Data Acquisition

We used a Bagnoli-8 sEMG system (Delsys, Inc.) to collect sEMG from the muscles of interest. Subjects' arms were lightly abraded with fine sandpaper then cleaned with isopropyl alcohol wipes prior to electrode placement following recommended procedures [19]. Agonist-antagonist muscle groups were chosen to provide sEMG data for the assistive torque. Channel 1 and channel 2 electrodes were placed over the center of the flexor carpi radialis (FCR) and extensor carpi ulnaris (ECU), respec-

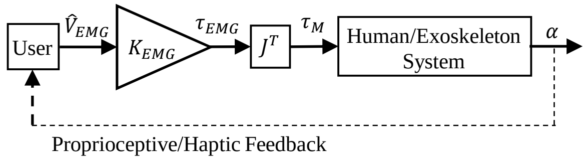

Figure 3. ASSISTIVE CONTROLLER, WHERE K_{EMG} IS AN ADJUSTABLE GAIN, τ_{EMG} IS THE FEED-FORWARD SEMG BASED TORQUE, J IS THE DEVICE JACOBIAN, τ_M IS THE TORQUE COMMANDED TO THE WRIST MOTORS AND α IS THE WRIST ANGLE.

tively. Throughout the experiment, the subject's angle of forearm pronation-supination was held constant by the exoskeleton handle. Subjects wore thin rubber gloves on their right hand and their right arms were wrapped in neoprene to reduce electromagnetic interference (EMI) from the exoskeleton. Additionally, each the subjects' right hand was wrapped using an elastic bandage around the MAHI Exo-II's handle to reduce recorded sEMG activity due to grip. The Delsys system provided an overall gain of 1000x and band pass filtering of 20-450 Hz. Real time code was developed in Simulink (The Mathworks, Inc) then compiled into C++ using Quarc software (Quanser Consulting, Inc.). The exoskeleton's data acquisition card (DAQ), a Q-8 USB (Quanser Consulting Inc), drove the exoskeleton while a Q-2 USB simultaneously recorded the sEMG data from the agonist-antagonist channels. The DAQ's sampled the encoder positions for each of the exoskeleton's five motors, three of which control the wrist parallel mechanism, provided current commands to the exoskeleton Accelus amplifiers (Copley Controls), and record the sEMG signal at 1 kHz. Another filtering stage was applied digitally using a 25-450 Hz band-pass, 8th order, Elliptic filter design to further remove exoskeleton EMI. Each channel was smoothed using a 300 ms running root mean square (RMS) calculation. Figure 2 shows the acquisition of the sEMG control signal after amplification and filtering.

sEMG Assistive Mode

The assistive mode is a feed-forward torque controller as shown in Figure 3. Feed-forward torque is calculated using the difference in sEMG power from agonist-antagonist muscle groups after each signal is normalized to a sub-maximal voluntary isometric contraction (SMVIC), $\Delta\hat{V}_{EMG}$. This normalization provides an estimated linear mapping between torque and sEMG. Although multiple muscles contribute to wrist movement in any direction, a configuration with single channel over the flexors or extensors for each movement direction was chosen for simplicity. The difference in normalized sEMG signals is then multiplied by a adjustable gain, K_{EMG}. Saturation limits in software prevented the wrist mechanism from providing more than 1 Nm of assistive torque for user safety.

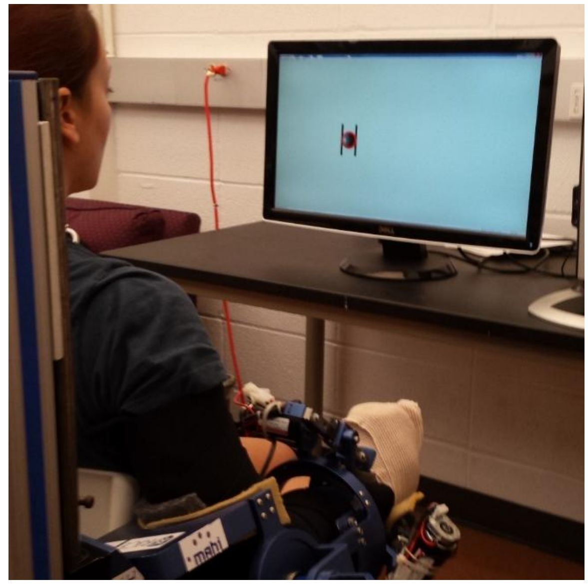

Figure 4. A SUBJECT HOLDS THE CURSOR OVER THE LEFT TARGET DURING THE TRACKING TASK.

Experimental Protocol

Six healthy subjects (three male, three female, ages 20-30, right hand dominant) were recruited to participate, completing wrist movements with their right wrist. Subjects provided informed consent to this protocol which was approved by the Rice Institutional Review Board. The exoskeleton was then fit to the subject and center and extreme positions in the parallel mechanism's workspace were chosen as left and right targets during the experimental task. Each subject then completed a short calibration protocol that took approximately 90 s. Initially, 5 s of baseline data were recorded for the two channels with the subject resting while the exoskeleton held the subject in the center position. Next, the exoskeleton ramped up to a constant commanded torque for 5 s about the active DoF while sEMG data were recorded for channel 1 and the subject held a constant position. The mean signal power during the last 2 s were used to generate the SMVIC torque mapping. A visual display with a cursor corresponding to the current wrist position and a target corresponding to the center position were shown on screen along with signal traces for the two channels. Subjects were instructed to avoid co-contraction during the calibration by minimizing the displayed signal trace associated with the antagonist muscles while holding the cursor on the target by activating the agonist muscle. For the entire experiment, the calibration torque was 1 Nm and all inactive DoF were held in a fixed location. The exoskeleton then reversed the perturbation torque direction and repeated the calibration for the second direction, channel 2 as the agonist muscle.

Following calibration, subjects completed 10 movements

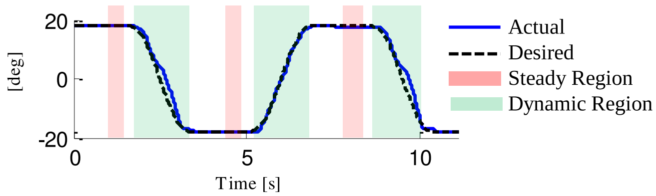

Figure 5. REGIONS OF THE TRACKING TASK FOR ANALYSIS.

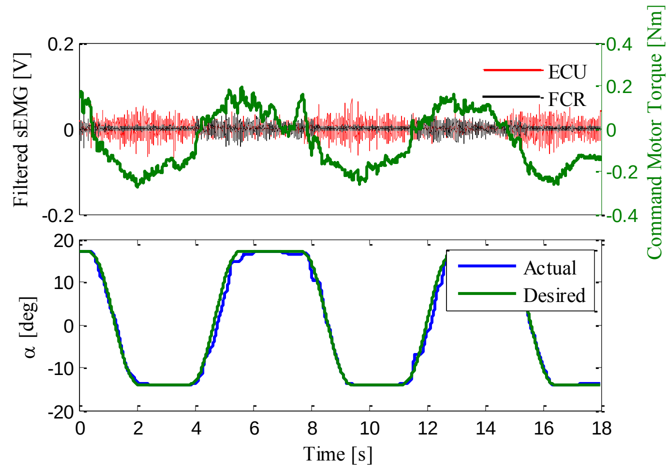

Figure 6. EXAMPLE FILTERED SEMG DATA AND COMMANDED ASSISTIVE TORQUE AND ASSOCIATED WRIST POSITION.

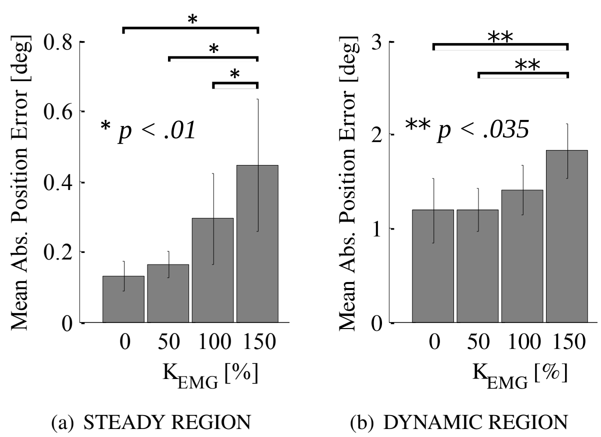

Figure 7. MEAN POSITION ERROR CALCULATED COLLAPSING ACROSS SUBJECTS. STANDARD ERROR SHOWN.

back-driving the exoskeleton to familiarize themselves with the visual interface. On the visual display, the target alternated between black and red to prompt the user to move to it while keeping a cursor corresponding to wrist position between two vertical bars as they moved between two targets (Figure 4). The goal trajectory was calculated using the minimum jerk profile [20] given 2 s to complete the movement. The target then remained for 1.5 s until the next target appeared at the opposite extreme of the workspace. The first experimental block consisted of 70 movements between a target at one extreme of the workspace to a target at the other extreme, while back-driving the exoskeleton. The subject then completed five more blocks of trials alternating between an experimental K_{EMG} condition (50%, 100%, 150%), and back-driving the exoskeleton. Order for condition was pseudo-randomized.

Data Analysis

Data from the first and last 20 movements in each experimental block, 10 movements in each direction, were selected for analysis. For each movement, data were split into two regions to assess performance with both a dynamic and steady target (Figure 5). The dynamic region extended from the time the target was presented until the subject arrived within a certain threshold of the target position, approximately 2 s. The steady region extended from 750 ms to 250 ms before the target switch, while holding at the extreme of the workspace. Mean absolute position error was calculated during each of these regions. The integral of EMG activity (iEMG) was calculated for the steady task in the fixed 500 ms window following post-post processing full wave rectification and 3 Hz low-pass filtering. The difference in performance from the first 20 movements was compared to the last 20 movements to investigate learning effects.

RESULTS

Data were analyzed using repeated measures ANOVA with a significance level of $\alpha = .05$. Two within subjects factors, movement direction and level of sEMG assistance, were investigated. Several example movements for one subject with $K_{EMG} = 100\%$ are presented in Figure 6. One subject was identified as a within subjects outlier (> 3 inter-quartile ranges from subject mean) in multiple metrics and removed from analysis. Figures 7(a) and 7(b) present results for position error. Significant effects of K_{EMG} were observed in the dynamic, $F(1.78, .001) = 10.45$, $p = .018$, $\eta_p^2 = .72$, and steady, $F(1.74, < .001) = 20.82$, $p = .001$, $\eta_p^2 = .84$, regions of the task. A Greenhouse-Geisser correction was applied. No significant effects of direction or interaction between K_{EMG} and direction were observed ($p > .49$). The effect of K_{EMG} was further analyzed using pairwise t-tests with a false discovery rate adjustment. Significant differences were only found in comparisons involving the highest level of K_{EMG}.

The difference in position error from the first 20 movements and last 20 movements was also investigated to assess learning. For the dynamic tracking task, no significant effect of K_{EMG} was found regarding the change in performance or interaction of K_{EMG} and direction ($p > .22$). Observing Figure 8(b), there appears to be minimal change in the no and low levels of K_{EMG} assistance condition but an improvement in performance for the

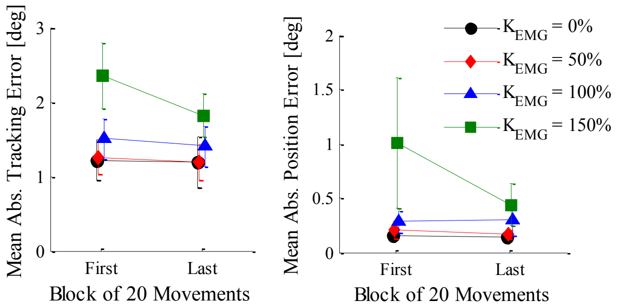

(a) STEADY REGION (b) DYNAMIC REGION

Figure 8. CHANGE IN POSITION ERROR BETWEEN THE FIRST AND LAST 20 MOVEMENTS IN A BLOCK. MEANS CALCULATED COLLAPSING ACROSS SUBJECTS, STANDARD ERROR SHOWN.

$K_{EMG} = 150\%$ condition. Observing the results for the steady state performance (Figure 8(a)) a similar effect of K_{EMG} appears to be present, although, again, it is not significant at the $\alpha = .05$ level ($p = .064$). No significant effect of direction or interaction of direction and K_{EMG} was observed ($p > .77$).

The iEMG was calculated to estimate muscular effort. No significant effect of K_{EMG} or interaction with direction ($p > .34$) was observed in the flexor channel (Figure 9(a)). Although not significant in the repeated measures ANOVA, it appears as if increasing the gain K_{EMG} reduced activation of the flexor channel while holding at the extreme position corresponding to extension. The effect of K_{EMG} appears to be more variable during flexion.

In the extensor channel, no significant effect of K_{EMG} was found although there was a significant interaction between K_{EMG} and movement direction, $F(1.78, 21.98) = 8.52$, $p = .014$, $\eta_p^2 = .68$. In all but one subject, the relationship between extensor activity during movement in the extension direction decreased monotonically with increasing K_{EMG}. In the flexion direction, the relationship varies subject to subject, although it appears the effect is minimal. This interaction, visible in Figure 9(b), was decomposed using a post-hoc linear interaction contrast with a Scheffé adjustment. A significant linear contrast was found, ($p = .01$) suggesting the slopes were different.

No significant effect K_{EMG} was found on difference in iEMG between the first block and last block of 20 movements ($p > .45$) nor were any significant trends observed.

DISCUSSION

The objective of this experiment was to assess the ability of healthy subjects to control and exploit an sEMG based assistive torque from the MAHI Exo-II during wrist flexion-extension. Regarding the performance metric, position error, subjects attained similar performance levels with low and moderate levels of sEMG assistance during the dynamic portion of the task.

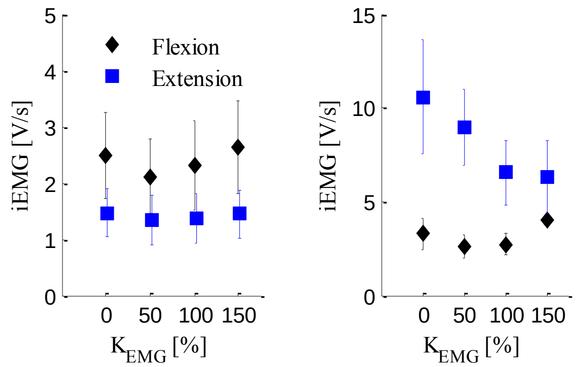

(a) FCR ACTIVITY (b) ECU ACTIVITY

Figure 9. RECORDED MUSCULAR ACTIVITY FOR FLEXION AND EXTENSION. STANDARD ERROR SHOWN.

While holding at the extremes of the workspace, position error increased with increasing levels of K_{EMG} with little change between back-driving the exoskeleton and $K_{EMG} = 50\%$. At this low level of assistance, it appears subjects were able to adapt and attain similar levels of performance to the no assistance condition. The only significant degradations in performance resulted at $K_{EMG} = 150\%$. Observing Figure 8(a), as subjects were improving in their ability to control the system, but it is unlikely they would have attained the same level of performance as the lower levels of K_{EMG}, subjects were not improving in the $K_{EMG} = 100\%$ condition. While interacting with a robotic system, healthy and impaired subjects are capable of adapting to predictable disturbances [21]. It is possible though, the increasing levels of K_{EMG} amplified biological noise and EMI surpassing the ability of the subject to reject unpredictable disturbances. For the proposed approach, the $K_{EMG} = 150\%$ condition resulted in a detrimental impact on performance. Future efforts will focus on distinguishing between environmental interference and biological motor noise to further reduce unpredictable disturbances.

Although decreases in iEMG were observed in the ECU, an average decrease of approximately 40% for $K_{EMG} = 100\%$ when compared to back-driving the exoskeleton across subjects, high variability prevented statistical significance. The reduction in recorded muscle activity, however, suggests a potential for this simplified approach. A reduction in muscular activity may be beneficial to rehabilitation as assistance may help reduce abnormal synergies in impaired populations [22]. Higher variability was observed in the FCR, although a trend of reduced sEMG activity is visible for the low and middle K_{EMG} conditions. This variability is likely explained by high motor system noise at low force levels [23]. Preliminary results from another experiment suggest healthy subjects completing a similar wrist flexion-extension movement while back-driving the exoskeleton only generated 2-5% of maximum voluntary isometric contraction sEMG activity. The only resistance to movement was low friction present in the device and elastic biological elements in the wrist, resulting in low contractile forces in these healthy subjects. Future work will include resistive forces during the tracking task to increase muscular activation in healthy subjects. In this protocol, five subjects did not provide sufficient power to resolve the observed differences in iEMG. For the conditions $K_{EMG} = 50\%$ and $K_{EMG} = 100\%$, antagonist muscle activation did not increase during the steady or dynamic task. Co-contraction is the natural method of increasing stability of performance, especially in unpracticed or unpredictable conditions [24], so co-contraction would be taken as evidence of a need to compensate for some difficulty in using the system. Therefore, absence of an increase in co-contraction in this task is evidence of an intuitive interface. Subjects were able to adapt to the sEMG assistance at the two lower levels of assistance with little or no impact on performance in a tracking task.

Conclusion

We explored the ability of healthy subjects to use sEMG based robotic assistance during a tracking task in wrist flexion-extension in order to validate the feasibility of this form of assistance with the MAHI Exo-II wrist exoskeleton. Low levels of sEMG assistance did not have significant impact on tracking performance. Although no significant differences were found in muscular activity, estimated from iEMG, overall we observed a trend of decreasing ECU activation with increasing sEMG assistance. Levels of co-contraction did not increase for the low levels of sEMG assistance, indicating that subjects did not feel a need to increase stability via co-contraction, therefore suggesting an intuitive interface. Further experiments will investigate simple sEMG assistance in the other MAHI Exo-II DoF and impaired populations. The controller can be used with other DoF, though for some DoF it may be limited by the amount of cross-talk from other muscle groups. We expect some differences in performance of impaired populations due to higher signal-to-noise ratios and higher levels of co-contraction; it is anticipated that changes in K_{EMG} will have a similar effect, but the magnitude of that effect may be smaller. This hypothesis remains to be tested in future work.

ACKNOWLEDGMENT

This work was supported in part by Mission Connect, a project of the TIRR Foundation, and NIH Grant 1R01NS081854.

REFERENCES

[1] Burns, A. S., and O'Connell, C., 2013. "Spinal cord injury facts and figures at a glance". *Spinal Cord,* ***36***(1).

[2] Curt, A., Van Hedel, H. J., Klaus, D., and Dietz, V., 2008. "Recovery from a spinal cord injury: significance of compensation, neural plasticity, and repair". *Journal of Neurotrauma,* ***25***(6), pp. 677–685.

[3] Riener, R., Nef, T., and Colombo, G., 2005. "Robot-aided neurorehabilitation of the upper extremities.". *Medical & Biological Engineering & Computing,* ***43***(1), Jan., pp. 2–10.

[4] Kwakkel, G., Wagenaar, R. C., Koelman, T. W., Lankhorst, G. J., and Koetsier, J. C., 1997. "Effects of intensity of rehabilitation after stroke a research synthesis". *Stroke,* ***28***(8), pp. 1550–1556.

[5] Zariffa, J., et al., 2012. "Relationship between clinical assessments of function and measurements from an upper-limb robotic rehabilitation device in cervical spinal cord injury". *IEEE Trans. Neural Sys. and Rehab. Eng.,* ***20***(3), pp. 341–350.

[6] Pehlivan, A. U., Sergi, F., Erwin, A., Yozbatiran, N., Francisco, G. E., and O'Malley, M. K., 2014. "Design and validation of the RiceWrist-S exoskeleton for robotic rehabilitation after incomplete spinal cord injury". *Robotica*.

[7] Fitle, K., Pehlivan, A. U., and O'Malley, M., Manuscipt in Press 2015. "A robotic exoskeleton for rehabilitation and assessment of the upper limb following incomplete spinal cord injury". *Intl. Conf on Robotics and Automation (ICRA) 2015*.

[8] Hogan, N., et al., 2006. "Motions or muscles? some behavioral factors underlying robotic assistance of motor recovery". *Journal of Rehabilitation Research and Development,* ***43***(5), p. 605.

[9] Blank, A. A., French, J. A., Pehlivan, A. U., and O'Malley, M. K., 2014. "Current trends in robot-assisted upper-limb stroke rehabilitation: promoting patient engagement in therapy". *Current Physical Medicine and Rehabilitation Reports,* ***2***(3), pp. 184–195.

[10] Dipietro, L., Ferraro, M., Palazzolo, J. J., Krebs, H. I., Volpe, B. T., and Hogan, N., 2005. "Customized interactive robotic treatment for stroke: Emg-triggered therapy". *IEEE Trans. Neural Sys. and Rehab. Eng.,* ***13***(3), pp. 325–334.

[11] De Luca, C. J., 1997. "The use of surface electromyography in biomechanics". *Journal of Applied Biomechanics,* ***13***, pp. 135–163.

[12] Loconsole, C., Dettori, S., Frisoli, A., Avizzano, C. A., and Bergamasco, M., 2014. "An emg-based approach for on-line predicted torque control in robotic-assisted rehabilitation". In Haptics Symposium (HAPTICS), 2014, IEEE, pp. 181–186.

[13] Kiguchi, K., Tanaka, T., and Fukuda, T., 2004. "Neuro-fuzzy control of a robotic exoskeleton with emg signals". *Fuzzy Systems, IEEE Transactions on,* ***12***(4), pp. 481–490.

[14] Pau, J. W., Xie, S. S., and Pullan, A. J., 2012. "Neuromuscular interfacing: establishing an emg-driven model for the

human elbow joint". *Biomedical Engineering, IEEE Transactions on,* ***59***(9), pp. 2586–2593.

[15] Lenzi, T., De Rossi, S. M. M., Vitiello, N., and Carrozza, M. C., 2012. "Intention-based emg control for powered exoskeletons". *Biomedical Engineering, IEEE Transactions on,* ***59***(8), pp. 2180–2190.

[16] Jiang, N., Englehart, K. B., Parker, P., et al., 2009. "Extracting simultaneous and proportional neural control information for multiple-dof prostheses from the surface electromyographic signal". *Biomedical Engineering, IEEE Transactions on,* ***56***(4), pp. 1070–1080.

[17] Pehlivan, A. U., Celik, O., and O'Malley, M. K., 2011. "Mechanical design of a distal arm exoskeleton for stroke and spinal cord injury rehabilitation". *IEEE Intl. Conf. on Rehab. Robotics (ICORR)*, Jan.

[18] French, J. A., Rose, C. G., and O'Malley, M. K., 2014. "A robotic exoskeleton for rehabilitation and assessment of the upper limb following incomplete spinal cord injury". *ASME 2014 Dynamic Systems and Control Conference*.

[19] Konrad, P., 2005. "The abc of emg". *A practical introduction to kinesiological electromyography,* ***1***.

[20] Flash, T., and Hogan, N., 1985. "The coordination of arm movements: an experimentally confirmed mathematical model". *The journal of Neuroscience,* ***5***(7), pp. 1688–1703.

[21] Patton, J. L., Stoykov, M. E., Kovic, M., and Mussa-Ivaldi, F. A., 2006. "Evaluation of robotic training forces that either enhance or reduce error in chronic hemiparetic stroke survivors". *Experimental Brain Research,* ***168***(3), pp. 368–383.

[22] Stein, J., Narendran, K., McBean, J., Krebs, K., and Hughes, R., 2007. "Electromyography-controlled exoskeletal upper-limb–powered orthosis for exercise training after stroke". *American Journal of Physical Medicine & Rehabilitation,* ***86***(4), pp. 255–261.

[23] Hamilton, A. F. d. C., Jones, K. E., and Wolpert, D. M., 2004. "The scaling of motor noise with muscle strength and motor unit number in humans". *Experimental Brain Research,* ***157***(4), pp. 417–430.

[24] Latash, M. L., 2010. "Motor synergies and the equilibrium-point hypothesis". *Motor Control,* ***14***(3), p. 294.